A snake robot joint mechanism with a contact force measurement system

Pål Liljebäck, Sigurd Fjerdingen, Kristin Y. Pettersen, and Øyvind Stavdahl

Abstract— **A snake robot can traverse cluttered and irregular environments by using irregularities around its body as push-points to aid the propulsion. This is denoted *obstacle-aided locomotion* and requires the snake robot to have two features: 1) a smooth exterior surface combined with 2) a contact force sensing system. These two features are characteristic of biological snakes, but have received limited attention in snake robot designs so far. This paper presents a joint mechanism for a snake robot aimed at meeting both these requirements. The paper details the design and implementation of the joint mechanism and presents experimental results that validate the function of the contact force measurement system.**

I. Introduction

Inspired by biological snake locomotion, snake robots carry the potential of meeting the growing need for robotic mobility in unknown and challenging environments. These mechanisms typically consist of serially connected modules capable of bending in one or more planes. The many degrees of freedom of snake robots provide traversability in irregular environments that surpasses the mobility of the more conventional wheeled, tracked and legged forms of robotic mobility.

The unique feature of snake robot locomotion compared to other forms of robotic mobility is that irregularities on the ground are actually beneficial for the propulsion since they provide push-points for the snake robot. While *obstacle avoidance* is an important topic for wheeled, tracked and legged robots, the goal of snake locomotion is rather *obstacle exploitation*. The term *obstacle-aided locomotion* was introduced by Transeth *et al.* [1] and captures the essence of this concept.

A variety of snake robot designs have been developed so far. Hirose developed the world's first snake robot as early as 1972 [2]. This snake robot was equipped with passive wheels along its body. The use of passive wheels enables a snake robot to achieve propulsion on flat surfaces by propagating horizontal waves backwards along its body, and is a feature exploited by several other wheeled snake robots [3], [4]. Snake robots without wheels also exist [1], [5]–[9]. To the authors' best knowledge, the works in [1], [6] present the only published experimental results concerning obstacle-aided locomotion with wheel-less snake robots. Obstacle-aided locomotion with wheeled snake robots have been studied in [2], [10].

The authors of this paper believe that a snake robot needs two distinct features in order to successfully demonstrate obstacle-aided locomotion in an unknown and cluttered environment. These are characteristic features of biological snakes, but have received limited attention in snake robot designs so far. The first requirement is a *smooth exterior surface* along the body of the snake robot that will allow the snake to glide forward as a result of the external forces acting on the body. Any irregularities along the body will potentially obstruct the locomotion when the snake robot glides across an irregular surface. The second requirement is a *contact force sensing system*. Contact force sensing allows the robot to detect when the body is in contact with a push-point and also control the force exerted on a push-point. Since the sum of contact forces along the snake body is what propels the snake forward, the ability to measure these forces is important in order to control the propulsion.

This paper presents a joint mechanism for a snake robot aimed at meeting both the requirements listed above, i.e. a smooth exterior surface combined with a contact force sensing system. The paper details the design and implementation of the joint mechanism and presents experimental results that validate the function of the contact force measurement system.

The paper is organized as follows. Section II gives a short overview of the snake robot design. Section III presents the actuation mechanism of the joint. Section IV describes how a smooth exterior surface is achieved. Section V describes the contact force measurement system. Section VI describes the control system. Section VII presents experimental results concerning the contact force measurement system, and finally Section VIII presents concluding remarks.

II. Overview of the snake robot design

As argued in the previous section, a snake robot needs a smooth exterior surface and a contact force sensing system in order to demonstrate intelligent obstacle-aided locomotion in unknown and cluttered environments. The joint mechanism presented in this paper has been developed to meet both these requirements. The idea is to encapsulate each joint by a spherical shell that gives the joint a smooth outer surface no matter how the joint is flexed. Contact force sensing is achieved by mounting force sensors underneath the spherical shell, which ideally will enable the the snake robot to measure contact forces applied anywhere on its surface. The resulting snake robot, illustrated in Fig. 1, will in other words consist of a serial connection of ball-shaped joint modules. The outer smoothness of the snake may be increased by inserting a hollow cylinder between each ball. The joint mechanism design is detailed in the following sections.

Pål Liljebäck, K. Y. Pettersen, and Øyvind Stavdahl are with the Department of Engineering Cybernetics at the Norwegian University of Science and Technology, NO-7491 Trondheim, Norway. E-mail: Pal.Liljeback@sintef.no, {Kristin.Y.Pettersen, Oyvind.Stavdahl}@itk.ntnu.no

Sigurd Fjerdingen is with SINTEF ICT, Dept. of Applied Cybernetics, N-7465 Trondheim, Norway. E-mail: Sigurd.Fjerdingen@sintef.no

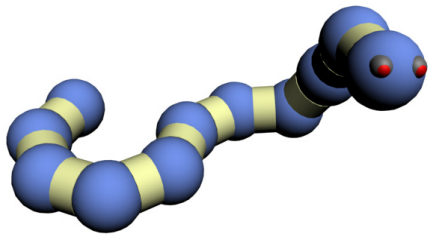

Fig. 1. Illustration of snake robot composed of ball-shaped joint modules. Hollow cylinders between each ball increase the outer smoothness of the snake.

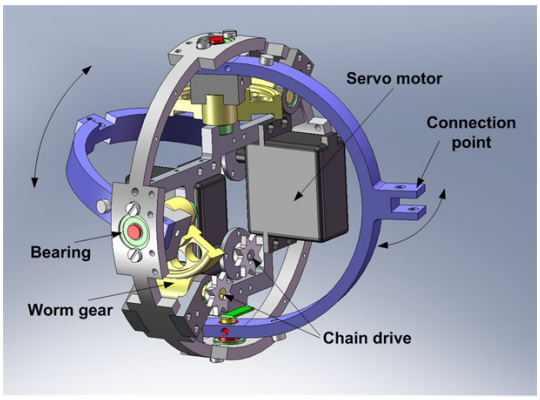

Fig. 2. Illustration of the articulation mechanism for the joint module.

III. Joint Actuation Mechanism

As illustrated in Fig. 2, the articulation mechanism of the joint module has two degrees of freedom and consists of two links supported by bearings in a steel ring. The outer diameter of the steel ring is 130 mm. Each link has a connection point at its centre that allows it to be connected to the next joint module by two screws. The axes of rotation of the two links are orthogonal and intersecting.

The angle of the two moving links in the joint are measured with magnetic rotary encoders (AS5043 from austriamicrosystems). A magnet with a 6 mm diameter is attached two each link so that it rotates above the rotary encoder as shown in Fig. 3. The encoders are attached to custom-designed circuit boards described in more detail in Section VI.

The motion of each link is powered by a Hitec servo motor (HS-5955TG) by connecting the output shaft of each motor to a worm gear (gear ratio of 1:5.71) through a steel roller chain. The worm gear and the chain drive are shown in Fig. 4 and Fig. 5. The servo motors are manufactured to have a limited range of rotation (about $\pm 90°$). However, the gearing between the motors and the links requires the motors to rotate more than this limited range. The motors were therefore manually modified in order to enable them to rotate continuously. The process of modifying the servos is very simple and consists of disconnecting the output shaft of the servo from its internal potmeter and also removing a mechanical pin inside the servo that otherwise would prevent the servo from rotating continuously.

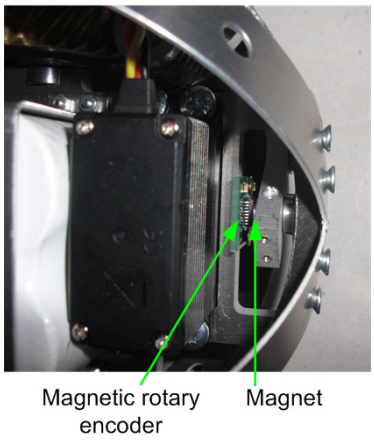

Fig. 3. Magnetic rotary encoder used for measuring the joint angle.

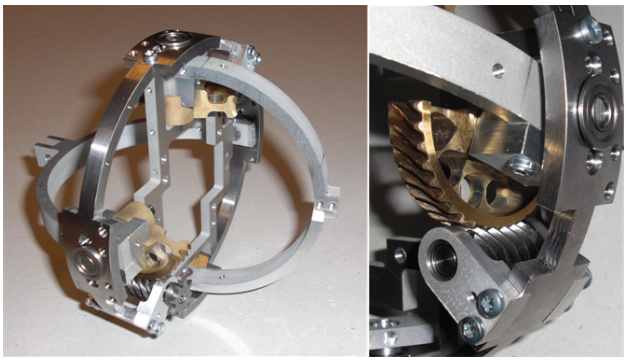

Fig. 4. The implemented articulation mechanism of the joint module.

Worm gears have a disadvantage due to a high friction component in the gear system. However, worm gears are advantageous in that they may essentially produce any desired gear ratio in a single gear stage. This facilitates a compact design. In addition, a worm gear is not likely to break in contrast to e.g. spur gears. This makes the joint mechanically robust. The steel roller chain between the servo motor and the worm gear is rated to handle forces significantly higher than the forces produced by the servo motor.

Experiments indicate that the servo motors produce a maximum continuous torque of about 1.6 Nm (at 6V supply voltage with a maximum current drain of about 3A). The rated power efficiency of the worm gears is about 75 %. This

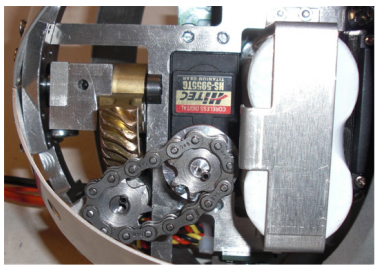

Fig. 5. Roller chain connecting the servo motor to the worm gear.

Parameter	Value
Total weight of joint	1.1 kg
Outer diameter	130 mm
Max joint travel	$\pm 50°$
Max continuous joint torque	4.5 Nm
Max joint speed (no load)	$70°/_{\text{sec}}$

TABLE I

PARAMETERS OF THE ACTUATION MECHANISM.

should theoretically give the joint mechanism a maximum continuous torque of around 7 Nm. However, experiments with the implemented joint mechanism indicate that the maximum continuous torque lies around 4.5 Nm. This is probably due to more friction in the worm gear than expected and also some friction in the chain drive. Table I lists the parameters characterizing the actuation system of the joint mechanism.

IV. EXTERIOR GLIDING SURFACE

The joint mechanism is covered by a spherical shell in order to give it a smooth outer surface. This is important to achieve gliding snake locomotion in irregular environments. The shell consists of two hemispherical parts. These two parts are not attached to the joint mechanism at any point, but are rather, to some extent, allowed to move with respect to the joint. The shell will, however, never detach from the joint since the joint is completely enclosed by the shell and the two hemispherical parts are firmly screwed together outside the joint. The motion of the shell with respect to the joint is somewhat constrained by the two links passing through the shell at the connection points to the two neighbouring joints. The reason for not attaching the shell to the joint mechanism is to allow for contact force measurements, which require that the force sensors represent the only connection points between the shell and the joint mechanism. The contact force measurement system is described in the next section.

The two hemispherical shells enclosing each joint have an outer diameter of 140 mm and were moulded from a plastic material. The shells are 2 mm thick and weigh 48 g each. As shown in Fig. 6, four aluminium plates are bent around the joint in order to support the shells and also to allow for contact force measurements.

The shells have a slit on each side corresponding to the range of motion of the connection points to the two neighbouring joints. This is illustrated in Fig. 7, which shows four connected joint modules. This figure also shows how a hollow cylinder of e.g. a plastic material may be mounted between each ball-shaped module in order to make the outer surface of the robot even more smooth. This solution will be implemented along with the development of the remaining joint modules for the snake robot.

V. CONTACT FORCE MEASUREMENT SYSTEM

A. Assumptions underlying the design

The purpose of the contact force measurement system is to enable the snake robot to conduct obstacle-aided locomotion, which requires the ability to detect contact forces along the snake body. The aim of the current snake robot design is

Fig. 6. Joint mechanism with spherical shell and support plates.

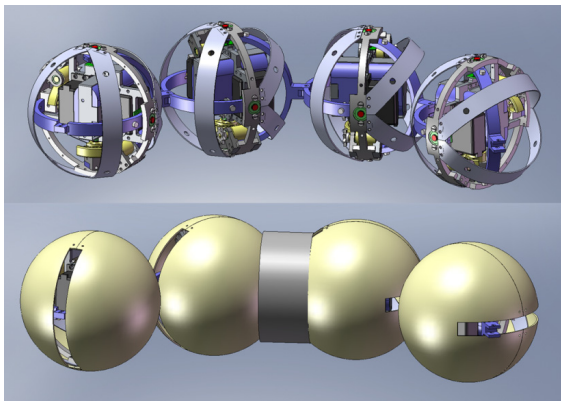

Fig. 7. Illustration of four connected joint modules.

to demonstrate *obstacle-aided locomotion on horizontal surfaces*. The current design therefore assumes that all contact forces are applied at the sides of the joint and not at the top or bottom. This assumption affects the placement of the contact sensors as shown later in this section.

The contact force measurement system has been developed to provide information about *contact forces with respect to the macroscopic shape of the snake robot*. Information about the specific location of an applied contact force within a single joint module is not believed to be of significant interest during obstacle-aided locomotion since force location within a single joint module only has a minor effect on the snake locomotion compared to force location with respect to the entire snake robot. This means that the sensor system is *only required to determine the magnitude of a contact force and also at which side of a joint module it is applied*, but not the specific location where the force is applied on the outer shell. It should be noted that information about

the force location within a joint module could be extracted from the force measurements by relating the magnitude of the measured forces to the relative placement of each sensor.

Assuming that the exterior surface of the spherical shell covering the joint is frictionless (which is obviously a crude approximation), the direction of any contact force will be normal to the spherical shell. Since the location of the contact force with respect to the shell is not determined by the sensor system, it will not be possible to determine the exact direction of the contact forces. However, as illustrated in Fig. 7, hollow cylinders will be mounted between each joint module in order to make the outer surface of the robot as smooth as possible. It is therefore believed that it will be adequate to *approximate the direction of any contact force as being normal to the macroscopic shape of the snake robot at the location where the force is applied.*

B. The sensor system setup

The four aluminium plates mounted around the joint shown in Fig. 6 allow contact force sensors to be mounted underneath the spherical shell. With a suitable arrangement of the force sensors, it is possible to detect and measure any force applied anywhere on the outer spherical surface of the joint. As explained in Section IV, the spherical shell is not attached in any way to the joint mechanism since contact force measurements require that the force sensors represent the only connection points between the shell and the joint mechanism.

A set of force sensing resistors (FSRs) are used to measure the external contact forces applied to the joint mechanism. A FSR is a polymer thick film device that exhibits a decrease in electrical resistance when the force applied to the active surface area of the sensor increases. Due to effects such as hysteresis, a FSR is not suited for precision measurements. However, the authors of this paper do not believe that obstacle-aided locomotion with a snake robot requires very precise force measurements. This, combined with its low cost and ease of use, make FSRs suitable as a force sensor on snake robots. The use of FSRs on snake robots for contact force sensing have previously been attempted in [5], [9].

The FSR used with the joint mechanism has a diameter (active sensor area) of 13 mm and is shown to the left in Fig. 8. The right of this figure shows how the FSRs are attached to the aluminium plates covering the joint. A small rubber pad (2.5 mm thick) is placed over the FSR in order to distribute forces across the entire active area of the sensor. An elastic rubber adhesive is used to attach the FSR and the rubber pad to the aluminium plate.

Note that the spherical shell enclosing the sensors is not completely rigid, i.e. the shell is, to some extent, deformable. This, combined with the deformability of the rubber pads placed over each FSR, means that there is compliance between the sensors and the location of an applied force. Compliance is necessary in order to measure the magnitude of the contact forces.

The placement of the sensors around the joint mechanism is shown in Fig. 9. Four FSRs are placed at each side of the joint in order to be able to measure horizontal contact forces, as explained in Section V-A. The specific placement of the FSRs around the joint is not critical since, as explained in the next section, the magnitude of the contact force is estimated by simply summing the contact forces measured at each FSR.

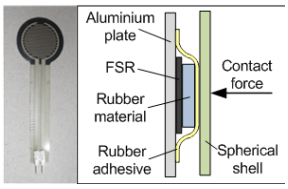

Fig. 8. FSR (Force sensing resistor) used to measure contact forces.

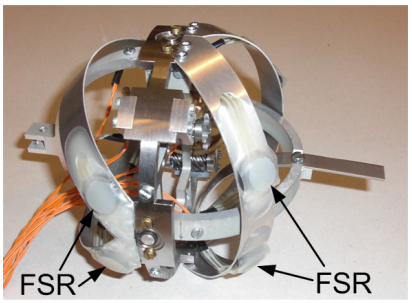

Fig. 9. Force sensors mounted to the joint mechanism.

The controller board for the joint, which is described in Section VI, contains a set of identical voltage divider circuits for measuring the resistance through the FSRs. The circuit diagram for the voltage divider circuit is shown in Fig. 10. The voltage V_{ADC}, where ADC denotes *analog to digital converter*, is the FSR measurement signal and is given as a function of the variable resistance across the FSR.

C. Force measurement

The force vs. resistance characteristic of a FSR is extremely nonlinear. However, as shown in Fig. 11, there is a near linear relationship between the conductance (1/resistance) of a FSR and the force applied to it. The measurements in the figure are indicated by '*' and were conducted with a FSR mounted as described in Fig. 8. A linear curve approximation to these measurements is plotted with a solid line in Fig. 11. The linear curve approximates the relationship between the force, F_{FSR}, applied to a FSR as a function of its conductance, G_{FSR}, and resistance, R_{FSR}. Based on the measurements, the expression for this linear curve was estimatet as

$$F_{\text{FSR}} = 18.9 \cdot G_{\text{FSR}} = \frac{18.9}{R_{\text{FSR}}} \tag{1}$$

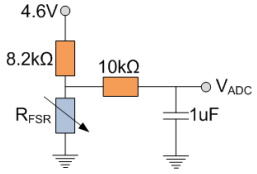

Fig. 10. Voltage divider circuit used to measure the resistance through the FSR.

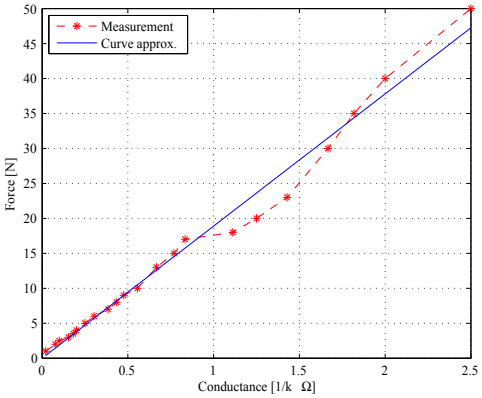

Fig. 11. The measured conductance (1/R) of the FSR as a function of applied force (measurements indicated by '*'). The solid line shows the linear curve approximation to these measurements.

A simple mapping may now be derived between the FSR measurement voltage in Fig. 10, V_{ADC}, and the estimated applied force, F_{FSR}. The measurement voltage is given by

$$V_{\text{ADC}} = \frac{R_{\text{FSR}}}{R_{\text{FSR}} + 8200} 4.6 \tag{2}$$

Solving (1) for R_{FSR}, inserting into (2), and solving for F_{FSR} give

$$F_{\text{FSR}} = \frac{4.6 - V_{\text{ADC}}}{8200 V_{\text{ADC}}} 18.9 \tag{3}$$

As shown in Fig. 9, each side of the joint mechanism is equipped with four FSRs. Since the spherical shell covering the joint mechanism is only in contact with the internal structure of the joint through the FSR measuring points, the magnitude of an external contact force applied to the joint may be estimated by simply summing the forces measured at each FSR. Denoting the four FSR measurements on the left side of the joint by $F_{\text{FSR,left},1}, .., F_{\text{FSR,left},4}$ and the measurements on the right side of the joint by $F_{\text{FSR,right},1}, .., F_{\text{FSR,right},4}$, the external forces, F_{left} and F_{right}, applied to the left and right side of the joint, respectively, are given by

$$\begin{aligned} F_{\text{left}} &= \sum_{i=1}^{4} F_{\text{FSR,left},i} \\ F_{\text{right}} &= \sum_{i=1}^{4} F_{\text{FSR,right},i} \end{aligned} \tag{4}$$

VI. Joint Control System

The joint mechanism is controlled by a custom-designed microcontroller board based on the Atmel microcontroller AT90CAN128. The board is shown to the left in Fig. 12. The right of this figure shows the magnetic rotary encoders used to measure the angle of the two links in the joint.

The function of the microcontroller board is illustrated in Fig. 13. In the complete snake robot, the board will continuously read angular measurements from the two encoders and also contact force sensor data from the FSRs. The board will also generate PWM pulses for controlling the two servo motors driving the joint. The board has a CAN bus interface for communicating with the other modules of the snake robot. The complete snake robot will have a brain module responsible for sending joint reference angles to all joint modules over the CAN bus.

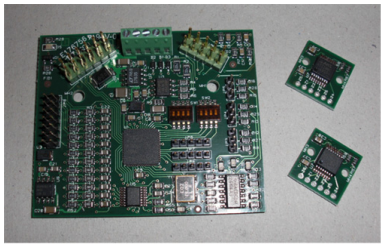

Fig. 12. Left: Microcontroller board developed to control the joint mechanism. Right: Magnetic rotary encoders for measuring the joint angle.

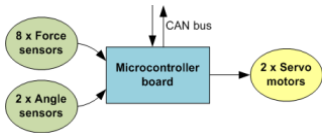

Fig. 13. Function of the microcontroller board of the joint mechanism.

The joint is powered by two serially connected Lithium Ion batteries from A123Systems of the type ANR26650M1. The batteries produce a supply voltage of about 6.6V at a capacity of 2.3Ah. The batteries were chosen due to their ability to deliver high currents (the maximum continuous discharge current is 70A) and also their short charge time (15 min charge time at 10A charge current). Each joint module in the complete snake robot will be equipped with a voltage regulator board and also a battery charger board that will allow the batteries in all the joint modules to be charged simultaneously by connecting the robot to an external power supply.

VII. Experimental Validation of the Contact Force Measurement System

This section presents experimental results that validate the ability of the joint mechanism to measure external contact forces from the FSR readings by use of (4). The experiment was conducted by holding the end points of the links and then manually pressing the joint mechanism against an external reference force sensor, as shown in Fig. 14. The forces from the reference sensor could then be compared with the forces estimated from the FSR readings. The reference force sensor used in the experiment is a force/torque sensor (Schunk FTC-050) originally developed for use on industrial robot manipulators. The sensor has a force measurement range of $\pm$300N and a rated accuracy of 5%. Note that a clamp was attached to the links of the joint in order to prevent them from moving during the experiment since the links were used as the support points for manually pressing the joint against the reference force sensor.

The joint mechanism was pressed against the reference sensor at 9 measuring points distributed uniformly across the side area of the joint as shown to the right in Fig. 15. The purpose of the experiment was to validate that the mechanism is capable of measuring forces applied anywhere in the area around the sides of the joint. The exact positions of the measuring points were therefore not considered to be important as long as the measuring points were appropriately distributed.

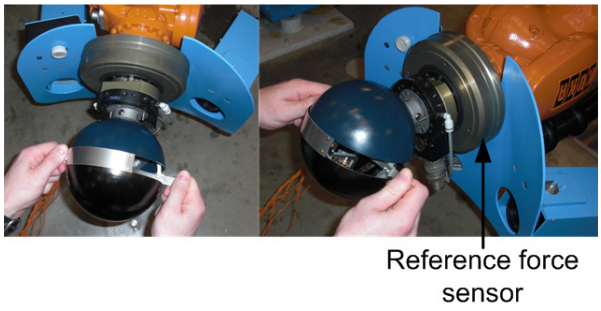

Fig. 14. The setup of the experiment conducted in order to test the contact force measurement system.

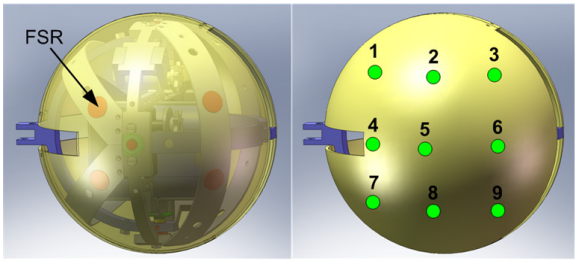

Fig. 15. The 9 predetermined measuring points that were pressed against the reference force sensor during the experiment.

Each measuring point was pressed against the reference force sensor three times during the experiment in order to produce a small, medium and large force, respectively. The results from the experiment are plotted in Fig. 16, which shows the amplitude of the contact forces applied to each of the 9 measuring points on the spherical shell. The solid line shows the forces estimated from the FSR readings by use of (4), while the dashed line shows the reference force measurements. The reference force was calculated as the amplitude of the total force measured along all three axes of the reference sensor.

The agreement between the FSR forces and the reference forces is satisfactory. There are some deviations, such as the medium force applied to measuring point 5, which is about 12N higher than the reference force. The deviations are caused by a number of factors, such as the fact that a FSR is not suitable for precision measurements (as described in Section V-B). Some deviations were therefore expected. However, the authors of this paper believe obstacle-aided locomotion with a snake robot primarily requires the ability to detect a contact force and also, to some extent, assess the magnitude of this force. The experimental results indicate that the proposed sensor setup is able to meet these requirements.

VIII. Concluding Remarks

This paper has presented a joint mechanism for a snake robot aimed at enabling the robot to demonstrate obstacle-aided locomotion in cluttered and irregular environments. The authors of this paper believe obstacle-aided locomotion requires a snake robot to have a smooth exterior surface (in order to glide across irregular surfaces) combined with

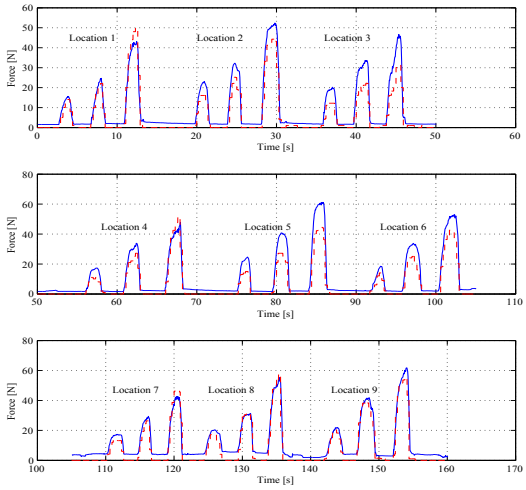

Fig. 16. Amplitude of a small, medium, and large contact force applied to each of the 9 measuring points on the spherical shell. Solid line: Force measurements from FSRs. Dashed line: Reference force measurements.

a contact force sensing system (in order to adapt to the environment). The joint mechanism presented in this paper incorporates both these features. The paper has detailed the design and implementation of the joint mechanism and has presented experimental results that validate the function of the contact force measurement system.

References

[1] A. A. Transeth, R. I. Leine, C. Glocker, K. Y. Pettersen, and P. Liljebäck, "Snake robot obstacle aided locomotion: Modeling, simulations, and experiments," *IEEE Trans. Robot.*, vol. 24, no. 1, pp. 88–104, February 2008.

[2] S. Hirose, *Biologically Inspired Robots: Snake-Like Locomotors and Manipulators*. Oxford: Oxford University Press, 1993.

[3] M. Mori and S. Hirose, "Three-dimensional serpentine motion and lateral rolling by active cord mechanism ACM-R3," in *Proc. IEEE/RSJ Int. Conf. Intelligent Robots and Systems*, 2002, pp. 829–834.

[4] H. Yamada, S. Chigisaki, M. Mori, K.Takita, K. Ogami, and S. Hirose, "Development of amphibious snake-like robot ACM-R5," in *Proc. 36th Int. Symp. Robotics*, 2005.

[5] P. Liljebäck, Ø. Stavdahl, and A. Beitnes, "SnakeFighter - development of a water hydraulic fire fighting snake robot," in *Proc. IEEE Int. Conf. Control, Automation, Robotics, and Vision*, Dec 2006.

[6] Z. Y. Bayraktaroglu, A. Kilicarslan, A. Kuzucu, V. Hugel, and P. Blazevic, "Design and control of biologically inspired wheel-less snake-like robot," in *Proc. IEEE/RAS-EMBS Int. Conf. Biomedical Robotics and Biomechatronics*, February 2006, pp. 1001–1006.

[7] H. B. Brown, M. Schwerin, E. Shammas, and H. Choset, "Design and control of a second-generation hyper-redundant mechanism," in *Proc. IEEE/RSJ Int. Conf. Intelligent Robots and Systems*, 2007, pp. 2603–2608.

[8] C. Wright, A. Johnson, A. Peck, Z. McCord, A. Naaktgeboren, P. Gianfortoni, M. Gonzalez-Rivero, R. Hatton, and H. Choset, "Design of a modular snake robot," in *Proc. IEEE/RSJ Int. Conf. Intelligent Robots and Systems*, 2007, pp. 2609–2614.

[9] S. A. Fjerdingen, J. R. Mathiassen, H. Schumann-Olsen, and E. Kyrkjebø, "Adaptive snake robot locomotion: A benchmarking facility for experiments," in *European Robotics Symposium 2008*, vol. 44, 2008, pp. 13 – 22.

[10] H. Date and Y. Takita, "Adaptive locomotion of a snake like robot based on curvature derivatives," in *Proc. IEEE/RSJ Int. Conf. Intelligent Robots and Systems*, San Diego, CA, USA, Oct-Nov 2007, pp. 3554–3559.